

# Ulysses jovian latitude scan of high-velocity dust streams originating from the jovian system

Harald Krüger<sup>a,\*</sup>, Amara L. Graps<sup>b</sup>, Douglas P. Hamilton<sup>c</sup>, Alberto Flandes<sup>d</sup>, Robert J. Forsyth<sup>e</sup>, Mihaly Horányi<sup>f</sup>, Eberhard Grün<sup>g,h</sup>

<sup>a</sup>Max-Planck-Institut für Sonnensystemforschung, 37191 Katlenburg-Lindau, Germany

<sup>b</sup>INAF-Istituto di Fisica dello Spazio Interplanetario, CNR - ARTOV, 00133 Roma, Italy

<sup>c</sup>University of Maryland, College Park, MD 20742-2421, USA

<sup>d</sup>Departamento de investigaciones solares y planetarias, Instituto de Geofísica, UNAM Ciudad Universitaria, Coyoacán 04510, Mexico City, Mexico

<sup>e</sup>The Blackett Laboratory, Imperial College, London SW7 2BZ, UK

<sup>f</sup>Laboratory for Atmospheric and Space Physics, University of Colorado, Boulder, Co, USA

<sup>g</sup>Max-Planck-Institut für Kernphysik, 69029 Heidelberg, Germany

<sup>h</sup>Hawaii Institute of Geophysics and Planetology, Honolulu, HI 96822, USA

Received 15 September 2005; accepted 4 May 2006

Available online 24 July 2006

## Abstract

In February 2004 the Ulysses spacecraft had its second flyby at Jupiter at 0.8 AU distance from the planet. Twenty-eight dust streams emanating from the jovian system were measured between November 2002 and August 2005 while the spacecraft was within 4 AU of the planet, scanning jovigraphic latitudes from  $+75^\circ$  to  $-25^\circ$ . The highest dust fluxes were measured in mid 2004 at the passage of the equatorial plane of the planet when more than 2000 impacts per day were measured. The grain impact direction is correlated with the polarity and strength of the interplanetary magnetic field. At high jovigraphic latitudes, the impact rates show a periodicity of 26 days, closely matching the solar rotation period, while at the jovian equator the streams fluctuate with twice this period. The 14-day subharmonic streams alternate in arrival direction and are correlated with the pointing of the interplanetary magnetic field. Dust fluxes measured above and below the equatorial plane roughly decrease with the inverse square of the distance from the planet while along the equatorial plane dust fluxes are enhanced by up to 2 orders of magnitude.

© 2006 Elsevier Ltd. All rights reserved.

**Keywords:** Interplanetary dust; Dust streams; Interplanetary magnetic field; Dust-plasma interaction; Planetary volcanism

## 1. Introduction

One of the most intriguing discoveries of the Ulysses mission so far has been the detection of periodic, collimated burst-like streams of high-velocity, submicron-sized dust particles during the spacecraft's encounter with Jupiter in 1992 (Grün et al., 1993). A total of eleven dust streams were measured during Ulysses' first encounter with Jupiter within 2 AU of the planet (Baguhl et al., 1993; Grün et al., 2001). The streams occurred at approximately monthly intervals ( $28 \pm 3$  days) which was a complete surprise because no periodic phenomenon was known

before for small dust grains in interplanetary space. The measured impact rates exceeded by up to 3 orders of magnitude the typical rates seen in interplanetary space before. The dust grains approached the spacecraft from close to the line-of-sight to Jupiter, suggesting an origin from the jovian system.

While the particles' approach directions were roughly along line-of-sight to Jupiter, most streams deviated somewhat from this direction implying that strong non-gravitational forces must have been acting on the grains (Grün et al., 1993). Such forces are also required for dust to escape the jovian system. Hamilton and Burns (1993) argued that the interplanetary magnetic field was responsible for the deviations, and tied the streams 14- and 28-day periodicities to solar rotation. More detailed analysis

\*Corresponding author. Tel.: +49 5556 979234; fax: +49 5556 979240.  
E-mail address: [krueger@mps.mpg.de](mailto:krueger@mps.mpg.de) (H. Krüger).

showed that the deviation from the Jupiter direction was correlated with the magnitude and direction of the interplanetary magnetic field (especially its tangential component, Grün et al., 1996a). Particle sizes derived from numerical simulations were extremely small,  $\sim 10$  nm, and the particle speeds exceeded  $200 \text{ km s}^{-1}$  (Zook et al., 1996).

In 1995, the Galileo spacecraft confirmed the jovian dust streams: dust “storms” with up to 10 000 impacts per day were recorded in interplanetary space within 0.5 AU from Jupiter (Grün et al., 1996a). Between 1996 and 2002, Galileo continuously monitored the streams in the jovian system (Krüger et al., 2005) and revealed strong particle interaction with Jupiter’s magnetic field (Grün et al., 1996b, 1997a, 1998): the corotating electric field leads to acceleration and ejection of the small grains from the planet’s magnetosphere if they carry a net positive charge (Horányi et al., 1993a,b; Horányi et al., 1997; Hamilton and Burns, 1993). The Galileo long-term measurements finally identified Io as the major grain source (Graps et al., 2000) and it was shown that the dust streams can serve as a monitor for Io’s volcanic activity (Krüger et al., 2003).

The Cassini flyby at Jupiter in 2000/2001 offered the unique opportunity for compositional analysis of the jovian stream particles: between September 2000 and May 2001 (while Cassini was within 2 AU from Jupiter) a total of 458 grains were chemically analysed (Postberg et al., 2006). Sodium, potassium, sulfur and possibly silicon were identified, species which are compatible with a grain origin from Io’s volcanoes.

Recently, the saturnian system also turned out to be a source for high-speed grains: during approach to Saturn in 2004, the dust detector on board Cassini measured dust streams within 0.4 AU from the planet (Kempf et al., 2005). The reported speeds exceed  $100 \text{ km s}^{-1}$  and the most plausible grain sources are Saturn’s A and E rings. Grain sizes may be below 10 nm, probably smaller than the jovian particles.

In February 2004—almost exactly 12 years after its initial Jupiter flyby—Ulysses approached the planet Jupiter a second time, and had a closest approach distance of 0.8 AU. The first new Ulysses dust stream was detected in November 2002 when the spacecraft was still 3.4 AU away from the planet. Because Ulysses’ orbital plane is almost perpendicular to the ecliptic plane, the streams could be measured over a large range in jovigraphic latitude  $\beta_J$  from Jupiter’s north polar region down to just below the jovian equator ( $75^\circ > \beta_J > -25^\circ$ ). These data nicely supplement the Ulysses stream measurements of 1991/92 obtained with  $-35^\circ \leq \beta_J \leq 0^\circ$ .

Although the Ulysses dust measurements from the first Jupiter flyby of 1991/92 and the later Galileo measurements imply particle interaction with the interplanetary magnetic field, the details of this process are still poorly known. The Ulysses data from the Jupiter distant encounter in 2004 offer an additional opportunity for an investigation of this process, as this data set more than doubles the number of measured streams and samples

jovigraphic latitudes never before visited. In this paper we analyse the Ulysses dust measurements from this time interval, together with magnetic field data also obtained with Ulysses (Jones and Balogh, 2003) in order to elucidate the interaction of the dust grains with the interplanetary magnetic field.

## 2. Ulysses dust detection

### 2.1. Spacecraft trajectory

The Ulysses spacecraft was launched in October 1990. A swing-by manoeuvre at Jupiter in February 1992 rotated the orbital plane  $79^\circ$  relative to the ecliptic plane, and put the spacecraft onto an orbit with aphelion at 5.4 AU and a six-year period. Subsequent aphelion passages occurred in April 1998 and June 2004; more details on the spacecraft and mission are given by Wenzel et al. (1992). Dust streams were detected around Ulysses’ 1992 and 2004 aphelia, but not in 1998 when Ulysses was at the same location in space and Jupiter was on the opposite side of the Sun. This provides clear additional evidence that the jovian system is the source of dust streams.

The Ulysses trajectory for the Jupiter encounter in 2004 is shown in Fig. 1. During its approach to Jupiter from 2001 to mid 2004, the spacecraft was on the northern part of its out-of-ecliptic trajectory. The highest northern declination w.r.t. the jovian equator (jovigraphic latitude) of  $\beta_J = +75.5^\circ$  was reached on 20 November 2003 (Fig. 2). During its closest approach to Jupiter on 5 February 2004, the spacecraft was still at  $\beta_J = +50^\circ$ , and the passage through the jovian equatorial plane occurred on 8 June 2004. Five weeks later, on 14 July 2004, the spacecraft crossed the ecliptic plane and began approaching the Sun at southern ecliptic latitudes again. Since July 2004, Ulysses’ jovigraphic latitude has been slowly decreasing.

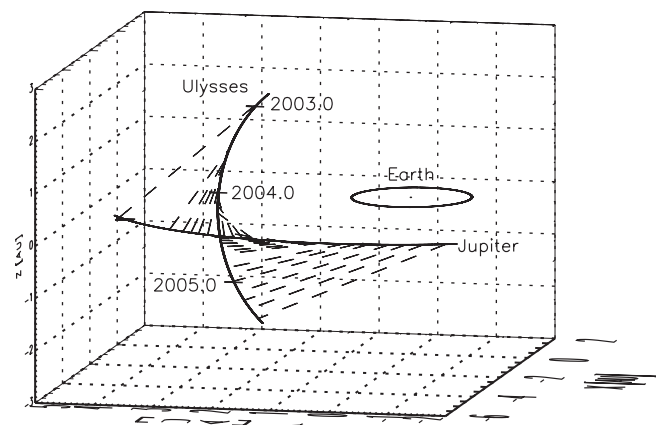


Fig. 1. The trajectories of Ulysses, Jupiter and Earth between late 2002 and mid 2005 in heliocentric coordinates, oblique view from above the ecliptic plane ( $X$ – $Y$  plane). Vernal equinox is towards the positive  $X$  direction and North is at the top ( $+Z$  direction). Dashed lines connect the positions of Jupiter and Ulysses when dust streams were detected. The spacecraft spin axis was always pointing towards Earth and, hence, as a first order approximation the dust detector scanned in the  $Y$ – $Z$  plane.

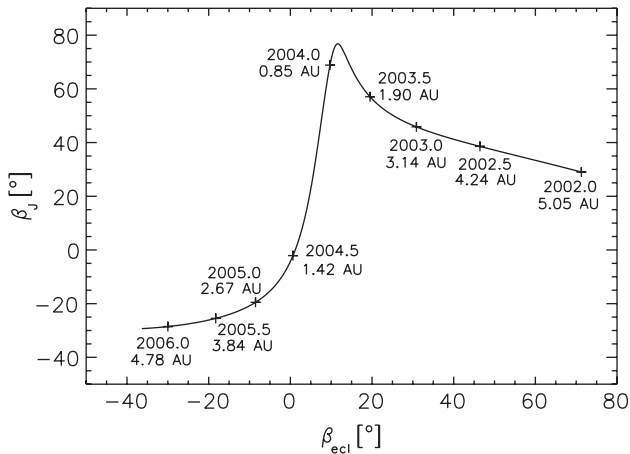


Fig. 2. Ulysses' jovigraphic latitude  $\beta_J$  vs. ecliptic latitude  $\beta_{\text{ecl}}$ . The distance from Jupiter  $r_J$  is indicated for times at half year intervals. "200 × .0" and "200 × .5" denote 01 January and 01 July of year 200×, respectively.

Between October 2003 and June 2004, the joviocentric distance changed relatively little between 0.8 and 1.3 AU, however, the latitude varied over almost the entire northern jovian hemisphere ( $+75^\circ \geq \beta_J \geq 0^\circ$ ), thus scanning over a large latitude range with only little variation in joviocentric distance. This geometry provides a unique data set for investigating jovian dust streams.

## 2.2. Dust detector

Ulysses spins at a rate of five revolutions per minute about the centre line of its high gain antenna, which normally points towards Earth. The highly sensitive impact ionisation dust detector on board measures impacts of dust grains onto its sensor target (Grün et al., 1992a). The dust sensor has a  $140^\circ$  wide field-of-view with a sensor area of  $1000 \text{ cm}^2$  and it is mounted at the spacecraft nearly at right angles ( $85^\circ$ ) to the antenna axis (spacecraft spin axis). Due to this mounting geometry, the sensor is most sensitive to particles approaching from the plane perpendicular to the spacecraft–Earth direction. The impact direction of dust particles is measured by the rotation angle  $\theta$ , which is the sensor viewing direction at the time of a dust impact. During one spin revolution of the spacecraft the rotation angle scans through a complete circle of  $360^\circ$ . It is measured in a right-handed system and  $\theta = 0^\circ$  is defined to be the direction closest to ecliptic north. At high ecliptic latitudes, however, the sensor pointing at  $\theta = 0^\circ$  significantly deviates from the actual north direction. During the passages over the Sun's polar regions, the sensor always scans through a plane tilted by about  $30^\circ$  from the ecliptic plane and all rotation angles lie close to the ecliptic plane (see e.g. Fig. 4 in Grün et al., 1997b). A sketch of the viewing geometry around aphelion passage can be found in Fig. 9.

The Ulysses dust instrument has been calibrated in the laboratory. Particle impact speeds and masses are derived from the rise times and amplitudes of the charge signals

measured upon impact onto the detector target. The calibrated range covers  $2\text{--}70 \text{ km s}^{-1}$  in impact speed and  $10^{-9}\text{--}10^{-19} \text{ kg}$  in particle mass (Grün et al., 1995). Uncertainties for the velocity—in the calibrated range—are a factor of 2, and, for the mass, a factor of 10. Our standard data analysis implied masses and speeds of the stream particles in the range  $10^{-19} \text{ kg} \leq m \leq 9 \times 10^{-17} \text{ kg}$  and  $20 \text{ km s}^{-1} \leq v \leq 56 \text{ km s}^{-1}$ , respectively. Assuming an average density of  $1 \text{ g cm}^{-3}$  the derived particle sizes were  $0.03\text{--}0.3 \mu\text{m}$ . However, numerical simulations of the grain dynamics (Zook et al., 1996) demonstrated that the grains in the streams are much smaller and faster than implied by the laboratory calibration of the instrument: grain radii were actually about  $10 \text{ nm}$  and their speeds exceeded  $200 \text{ km s}^{-1}$ . Since the dust instrument was not calibrated in this range there is considerably more uncertainty in measured masses and speeds and we must rely to some extent on theoretical modelling. Recent results from laboratory experiments show that the sensor side walls are as sensitive to dust impacts as the target itself. While relaxing directional constraints, they are not likely to significantly change our conclusions on grain sizes and speeds (Willis et al., 2005).

## 3. Dust measurements from the Jupiter distant flyby

### 3.1. Dust streams identification

Fig. 3 gives an overview of the Ulysses dust stream measurements from 2002 to 2005. The top panel shows the particle impact rate where dust streams appear as individual spikes. Previous analysis has shown that—for stream particles—the charges  $Q_1$  generated during dust impact onto the target and subsequently measured at the ion collector grid of the instrument were generally below  $10^{-13} \text{ C}$  (Baguhl et al., 1993). Note that  $Q_1$  does not measure the charge carried by the dust particle itself.  $Q_1$  is the most suitable parameter for a general impact classification compared to the other charge signals because it is less affected by noise. Therefore, in this paper we consider only particles below this threshold in order to separate dust stream particles from other populations of interplanetary and interstellar dust. By far the majority of particles identified in the 2002 to 2005 dust streams data set are below this threshold.

A prerequisite for an analysis of dust streams from Jupiter is a reliable identification of individual streams. Due to the relatively small dust fluxes, we must deal with small number statistics. Hence, real increases in the dust impact rate must be reliably separated from statistical fluctuations of the background flux in interplanetary space. The method we use here was first employed by Oberst and Nakamura (1991) for impacts on the moon. Its application to the identification of the jovian dust streams in the 1991/92 Ulysses data set was described by Baguhl et al. (1993) and Grün (2001). We form time intervals by sliding a window with a fixed number of events,  $N$ , over the data set

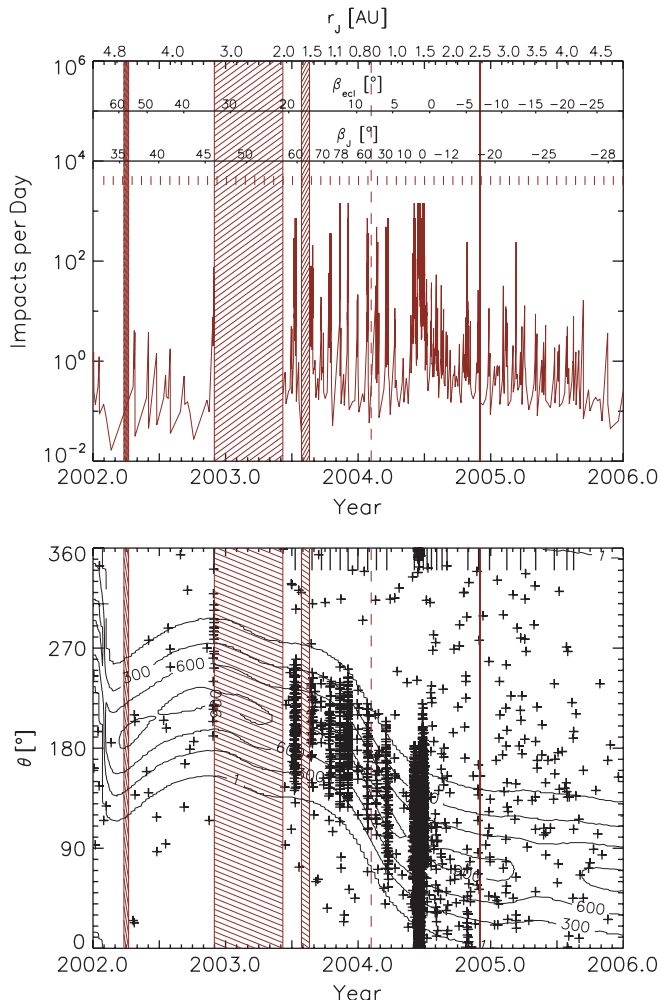


Fig. 3. Ulysses dust stream measurements from 2002 to 2005 (impact charges  $Q_1 \leq 10^{-13}$  C). Top panel: impact rate. No smoothing was applied to the data. The distance  $r_j$  from Jupiter, ecliptic latitude  $\beta_{\text{ecl}}$  and declination  $\beta_j$  w.r.t. Jupiter (jovigraphic latitude), respectively, are shown at the top. Short vertical dashes indicate the solar rotation period. A vertical dashed line shows Jupiter closest approach on 5 February 2004 and four grey shaded areas indicate periods when the dust instrument was switched off. Bottom panel: impact direction (rotation angle  $\theta$ ; ecliptic north is at  $\theta = 0^\circ$ ). Each cross indicates an individual dust particle impact. Contour lines show the effective dust sensor area for particles approaching from the line-of-sight direction to Jupiter and vertical dashes at the top indicate the dust streams.

and use Poisson statistics to calculate the probability that these impacts are due to a random fluctuation. A minimum in the probability function below a given level indicates a stream. We chose a probability of  $p_{\text{th}} = 10^{-4}$  as a detection threshold for a stream. Hence, the probability that dust impacts we identify as a stream are in reality caused by random fluctuations is below 0.01%.

A summary of the stream parameters is given in Table 1. For  $N = 8$  a total of 28 streams are identified between November 2002 and August 2005. Note that the number of impacts in a stream depends on  $N$  and the identification level  $p_{\text{th}}$ . Therefore, the number of stream particles and the

duration of streams have significant uncertainties. In particular, a less stringent identification level leads to the identification of more streams. Note that no speeds and masses of particles are given in Table 1 because they are outside the calibrated range of the dust instrument (Zook et al., 1996).

### 3.2. Impact rates

Ulysses' first dust stream after 1992 was detected in November 2002, when the spacecraft was still 3.4 AU away from Jupiter (Table 1 and Fig. 3). Unfortunately, on 1 December 2002, while this very distant stream # 1 was still ongoing, the dust instrument was switched off for power saving on board the spacecraft. The instrument was not switched on again until six months later when Ulysses had already moved to within 2 AU of Jupiter, causing a significant loss of potential stream detections. The instrument was also shut down for three other much shorter intervals, as indicated by the shaded areas in Fig. 3 (exact dates are given by Krüger et al. (2006)).

During 10 of the identified 28 streams, the dust impact rates exceeded 100 per day. In summer 2004, a particularly strong dust burst occurred with rates above 2000 per day (Fig. 4), containing many more particle impacts than all of the other streams combined (Table 1). This dust burst was the strongest ever measured by Ulysses, and was exceeded only by the major Galileo event during approach to Jupiter in 1995.

Interestingly, this burst was detected close to the jovian equator at about 1.3 AU joviocentric distance. Near Jupiter closest approach of 0.8 AU, when the spacecraft was at  $\beta_j = +50^\circ$ , the rates were about an order of magnitude lower. Note that in the 2002–2005 interval, the dust impact rate varied by more than 4 orders of magnitude and the streams were continuously detected from 0.8 AU joviocentric distance out to beyond 4.0 AU.

Strong periodicities of the streams are evident in the top panels of Figs. 3 and 4: between mid 2003 and early 2004, the streams occurred with roughly the solar rotation period which is about 26 days. In mid 2004—when Ulysses was close to the jovian equatorial plane—the streams occurred at about half this period, while at the end of 2004 the period had doubled again. This behaviour was predicted by Hamilton and Burns (1993) and will be analysed further in Section 4.

Some fine structure is also evident in the impact rate measured in 2004 (Fig. 4, top panel): for example, stream # 11 around day 80 has a double peak structure with the two maxima being separated by about 7 days. Double or even triple peaks were also recorded for several streams in 2003.

### 3.3. Impact directions

Important information about the origin of the streams and the interaction of the grains with the interplanetary



Table 1

Parameters of dust streams identified in the Ulysses data set: stream identification number; year; day of year; number of particles  $n$ ; duration of stream  $\Delta t$ ; deviation from Jupiter direction  $\delta$  (Eq. (1)); stream width  $\Delta\theta$ ; heliocentric distance  $r$ ; jovicentric distance  $r_J$ ; jovigraphic latitude  $\beta_J$ ; ecliptic latitude  $\beta_{\text{ecl}}$

No.	Year	Day	$n$	$\Delta t$ (days)	$\delta$ (°)	$\Delta\theta$ (°)	$r$ (AU)	$r_J$ (AU)	$\beta_J$ (°)	$\beta_{\text{ecl}}$ (°)
1 <sup>a</sup>	2002	332.5	19	2.9	40	47	4.3	3.4	44	33
2	2003	192.0	140	6.6	−4	30	5.0	1.8	58	19
3	2003	238.1	36	5.5	5	39	5.1	1.5	64	16
4	2003	263.6	9	1.8	8	17	5.2	1.4	67	15
5	2003	288.3	53	7.5	−6	29	5.2	1.2	72	14
6	2003	315.7	102	1.2	−2	29	5.2	1.1	76	12
7	2003	337.5	200	2.7	8	28	5.3	0.9	76	11
8	2003	364.5	10	3.0	15	33	5.3	0.9	70	10
9	2004	025.6	49	4.1	13	33	5.3	0.8	57	8
10	2004	050.0	20	3.7	4	44	5.4	0.8	44	7
11	2004	080.2	98	8.1	29	33	5.4	0.9	29	6
12	2004	155.3	257	10	30	34	5.4	1.2	3	2
13	2004	169.7	4058	12	−31	28	5.4	1.3	0	1
14	2004	181.0	547	10	42	31	5.4	1.4	−2	1
15	2004	190.2	9	2.4	−19	47	5.4	1.4	−4	0
16	2004	202.0	13	3.0	60	61	5.4	1.5	−5	0
17	2004	215.8	15	6.9	−19	52	5.4	1.6	−7	−1
18	2004	231.0	7	6.0	67	62	5.4	1.8	−9	−2
19	2004	246.0	8	4.0	−43	46	5.4	1.8	−11	−3
20	2004	302.5	13	5.0	−46	35	5.4	2.2	−16	−5
21	2004	331.8	5	1.0	56	39	5.3	2.4	−18	−7
22	2004	362.3	4	1.2	24	81	5.3	2.6	−19	−8
23	2005	044.2	9	5.0	60	77	5.3	3.0	−21	−11
24	2005	082.6	5	3.9	130	58	5.2	3.2	−23	−13
25	2005	123.9	7	2.0	62	59	5.1	3.5	−24	−15
26	2005	175.3	10	3.0	85	38	5.0	3.8	−25	−17
27	2005	209.8	7	3.0	64	77	4.9	4.0	−26	−20
28	2005	228.6	8	4.0	53	49	4.9	4.1	−26	−21

<sup>a</sup>End of stream not detected because instrument switched off on 334.0 in 2002.

magnetic field can be gained from the measured impact directions of the particles. The rotation angle  $\theta$  for each dust impact is shown in the bottom panels of Figs. 3 and 4. Contour lines are superimposed which indicate the effective dust sensor area for particles approaching the spacecraft from the line-of-sight direction to Jupiter. Grains approaching on straight trajectories from a source in the Jupiter system should arrive from close to the line-of-sight direction to the planet, while the directions of particles interacting with the interplanetary magnetic field can differ significantly (Zook et al., 1996).

Many dust streams can easily be recognised as vertical bands lying approximately in the line-of-sight direction to Jupiter. A few streams, however, strongly deviate from this direction. This is particularly evident for stream # 1 measured at 3.4 AU from Jupiter in November 2002, and for the bursts detected in June/July 2004 (streams # 12–14). For each stream, the measured range in rotation angle scatters over more than 100°, consistent with the wide field-of-view of the dust sensor and the favourable spacecraft orientation for stream detection during this time.

For a more quantitative analysis of the stream directions, we show in Figs. 5 and 6 the deviation  $\delta$  of the average stream direction from the line-of-sight

direction to Jupiter:

$$\delta = \theta_J - \frac{1}{n} \sum_{i=1}^n \theta_i. \quad (1)$$

$\theta_J$  is the rotation angle of the direction closest to the line-of-sight to Jupiter and  $\theta_i$  are the rotation angles for all  $n$  dust impacts measured in a stream. Contamination with particles originating from populations other than the jovian streams cannot be excluded but should be minor, in particular for the stronger streams with at least 100 impacts per day.

Vertical error bars in Figs. 5 and 6 represent the  $1\sigma$  standard deviation of the measured rotation angle distribution, i.e. on average 68% of all impacts are represented by the bar. For a monodirectional stream the expected width  $\Delta\theta$  of the impact angle distribution depends on the angle of the dust impact direction w.r.t. the dust sensor axis and can range from 0° up to the maximum sensor opening angle of 140°. The average  $1\sigma$  width of the streams measured in 2002–2005 is  $37^\circ \pm 17^\circ$  (Table 1), close to the value expected for a statistically large number of dust impacts (Grün et al., 1992a). It indicates that the streams are collimated to within several degrees, consistent with the Galileo dust stream measurements obtained within

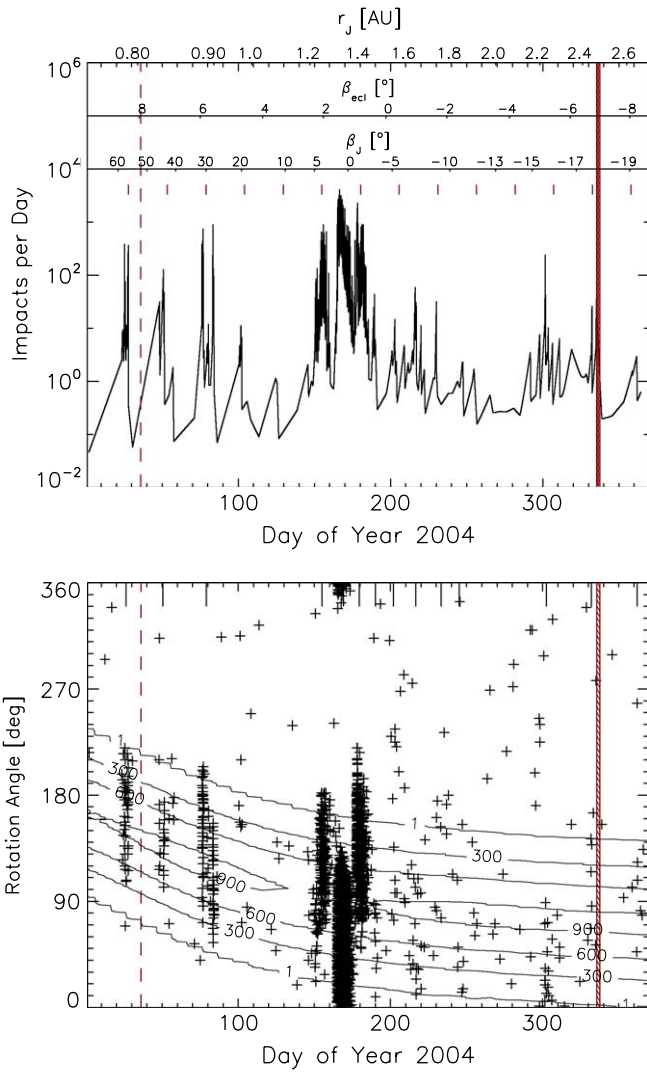


Fig. 4. Same as Fig. 3 but for 2004 only.

the jovian magnetosphere (Krüger et al., 1999). For streams with only a small number of impacts, the width can be significantly larger due to statistical variations or due to contamination from other dust populations. Some of the weaker streams have a much larger width while the strong streams are close to the nominal width.

Strong deviations from the line-of-sight direction to Jupiter are evident in Fig. 5. Particularly strong offsets are seen for the very distant stream # 1 measured in November 2002 ( $\delta = 40^\circ$ ) and for the streams seen in 2004 and 2005 (up to  $\delta = 130^\circ$ ). In 2003, on the other hand, the streams typically deviated by less than  $20^\circ$  from the Jupiter direction. Stronger deviations from the Jupiter direction occur at largest joviocentric distances (Fig. 5), consistent with the idea that electromagnetic forces have longer times to induce changes to the grain trajectories.

The impact directions for the streams measured in 2004 are shown in more detail in Fig. 6. The structure seen in the impact rate diagram also shows up in the impact direction: particularly obvious is a fluctuation from positive to

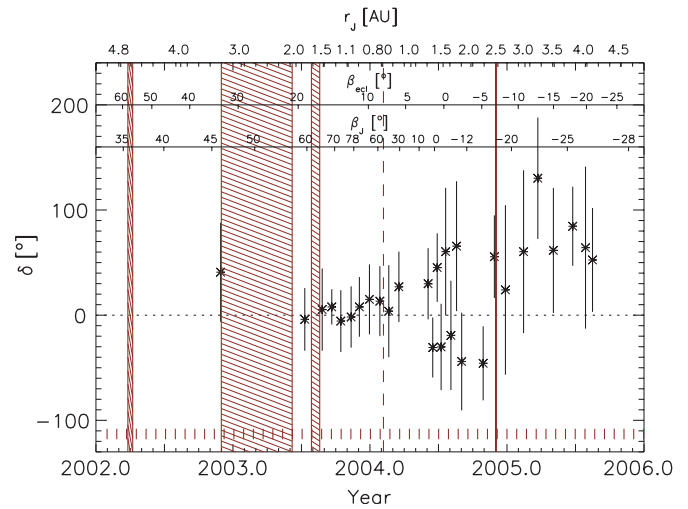


Fig. 5. Deviation  $\delta$  (Eq. (1)) of the average dust stream impact direction from the line-of-sight direction to Jupiter. Positive  $\delta$  refer to shifts towards larger rotation angles  $\theta$  (Fig. 3, bottom panel). Vertical bars represent the distribution of impact directions  $\Delta\theta$  measured for each individual dust stream. Note that the direction of the stream at the left edge of the large grey box may be biased because the full stream was not measured. Short vertical dashed lines at the bottom of the figure indicate the solar rotation period.

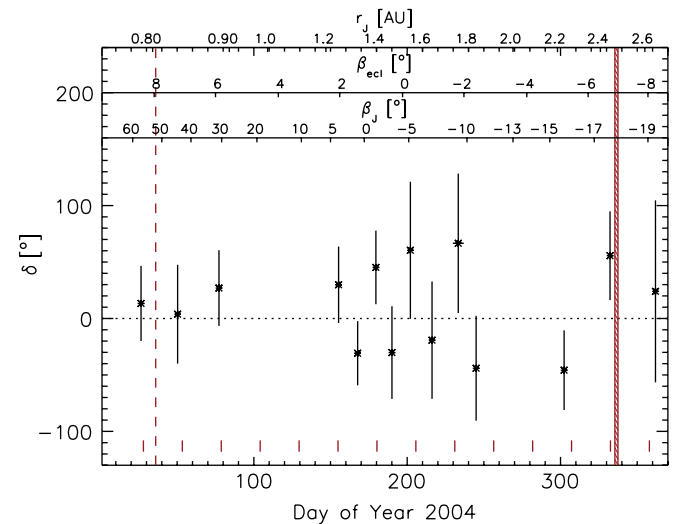


Fig. 6. Same as Fig. 5 but for 2004 only.

negative  $\delta$  from one stream to the next in mid 2004 which includes the burst between days 155 and 180. This variation was also seen in the 1992 Ulysses data and is expected theoretically with a 13-day periodicity by the model of Hamilton and Burns (1993). In early 2004, significant fluctuations occurred on even shorter timescales within some streams. In particular, the direction of the two maxima of stream # 11 on days 77–84 is shifted by  $41^\circ$  (Fig. 4). Finally, the average of the stream deviations for 2004,  $\bar{\delta} = \frac{1}{n} \sum_i^n \delta_i$  ( $i$  being the stream number), is  $\bar{\delta} \simeq 15^\circ$  towards the northern hemisphere while for 2003 the offset is  $\bar{\delta} \simeq 0^\circ$ . It indicates that in 2003 at high jovigraphic

latitudes—on average—the streams fluctuated around the Jupiter direction while at low latitudes within  $\pm 20^\circ$  of the jovian equator they were shifted to the north. We see almost no variation in  $\delta$  between mid 2003 and early 2004 when Ulysses was at high latitudes and relatively close to Jupiter while later there were strong fluctuations in the dust impact direction. Clearly Ulysses' changing detection geometry is playing a role here; we will return to address this point in Section 4.2, following a discussion of the electromagnetic forces responsible for deflecting the dust streams.

### 3.4. Dust streams fluxes

In Fig. 7 we investigate the dependence of the dust fluxes on jovicentric distance and latitude. For the flux calculation,

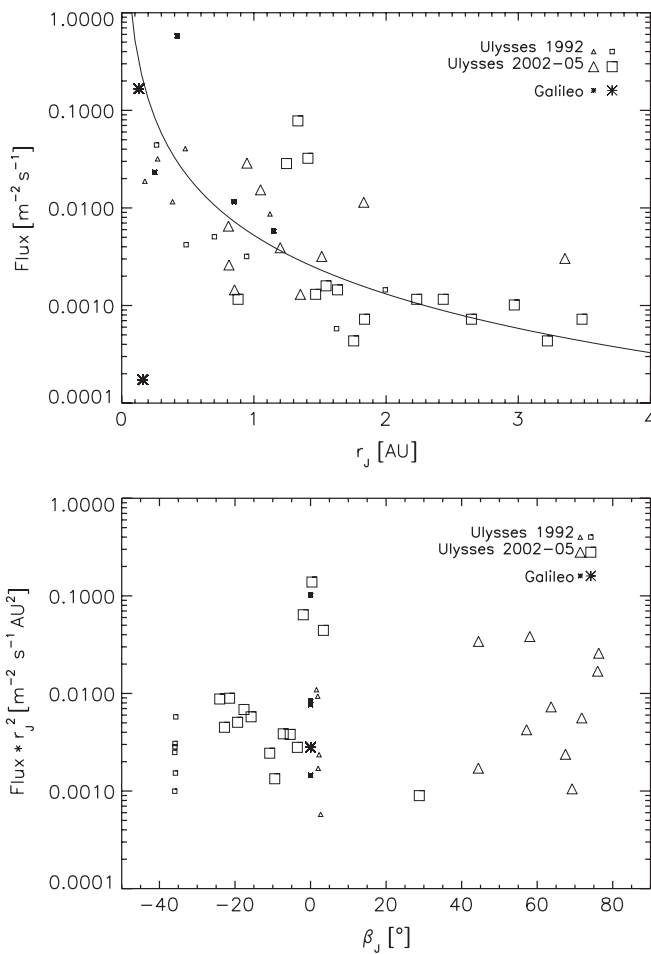


Fig. 7. Top panel: dust flux as a function of distance  $r_J$  from Jupiter. The solid line illustrates a drop in flux with the inverse square of the jovicentric distance. Bottom panel: normalised dust flux vs. jovigraphic latitude. The flux has been multiplied with the square of the distance to remove the dominant trend of flux variation with distance seen in the top panel. Each symbol represents a 4-day average of the measured flux. For Ulysses triangles show measurements during approach to Jupiter while squares show data obtained when Ulysses was moving away from the planet. For Galileo small symbols are measurements from 1995 when the spacecraft was approaching the planet while large symbols indicate measurements outside the jovian magnetosphere obtained in 2000 and 2002 (Krüger et al., 2005).

tion, we have assumed a spin-averaged effective dust sensor area of  $200 \text{ cm}^2$  (Grün et al., 1992b). The top panel shows a 4-day average of the dust fluxes measured with Ulysses and Galileo as a function of distance from Jupiter. The data show higher fluxes closer to the planet consistent with the expectation that closer to the source the flux should increase. For simple particle dispersion in space, the flux should drop with the inverse square of the distance from the source if the source strength remains constant. Ignoring the dust measurements obtained at low latitudes during the dust burst in mid 2004 (the three squares at  $r_J \approx 1.2\text{--}1.4 \text{ AU}$ ;  $r_J$  being the radial distance from Jupiter), the data are grossly consistent with this expectation. There is a clear trend of decreasing dust fluxes far from Jupiter with a rough  $r_J^{-2}$  dependence. It should be noted that Galileo measurements revealed variations by orders of magnitude within the jovian magnetosphere due to systematic and stochastic changes (Krüger et al., 2005). Thus, the Ulysses measurements imply that these fluctuations mostly smear out in interplanetary space far away from the planet.

The bottom panel of Fig. 7 shows the latitudinal variations of the measured dust fluxes. To remove—on average—the  $r_J^{-2}$  dependence of the fluxes, we have normalised the fluxes with the square of the jovicentric distance. The normalised fluxes do not show a strong variation with jovigraphic latitude, except in the equatorial plane of the planet. Here the fluxes are enhanced by 1–2 orders of magnitude compared to the region above or below the equatorial plane. The reasons for this increased dust flux are poorly understood, see Section 5. Galileo dust measurements obtained within the jovian magnetosphere monitored the dust emission of Io's volcanic plumes from 1996 to 2002 (Krüger et al., 2003). Elevated dust fluxes could be correlated with plume sightings and surface changes on Io. Assuming homogeneous dust ejection from the Io torus towards all jovian longitudes and towards latitudes of  $\pm 35^\circ$ , the derived average dust emission rate was  $0.1\text{--}1 \text{ kg s}^{-1}$ . Compared with  $\sim 10^3 \text{ kg s}^{-1}$  of plasma ejected from Io into the torus, the dust amounts to only 0.01–0.1% of the total mass released. While being a major dust source for the jovian system itself, Io is a minor source of interplanetary dust compared with comets and main belt asteroids ( $\sim 10^4 \text{ kg s}^{-1}$ ).

Estimates of Io's dust emission from the Ulysses measurements obtained in May/June 2004 at  $\approx 1.2\text{--}1.4 \text{ AU}$ —using the same assumptions—give unrealistically high dust production rates exceeding  $10^7 \text{ kg s}^{-1}$ . It clearly shows that this simple picture cannot be extrapolated into interplanetary space. From numerical simulations one expects particles to be transported to latitudes of  $\pm 25^\circ$  rather homogeneously (Horányi et al., 1997, Graps, 2001) while the measurements imply a much stronger concentration towards Jupiter's equatorial plane. On the other hand, groundbased observations showed strong volcanic activity on Io on 29 May 2004 (Marchis et al., 2004), coincident with the beginning of the strong dust burst measured with

Ulysses. Thus, the dust burst may indeed—at least partially—be connected with a sharp increase in Io’s dust emission.

### 3.5. Grain size variations

Laboratory calibration of the dust instrument has shown that the positive charge  $Q_1$  generated upon dust impact depends linearly on grain mass and much more steeply on its speed (Auer, 2001). Of all of the charge signals measured by the spacecraft, this is the most robust. From 2002–2005, the measured impact charges of most stream particles were in the fairly narrow range  $10^{-14} \text{ C} \leq Q_1 \leq 10^{-13} \text{ C}$ , the lower limit of this interval being the detection threshold of the instrument. Large impact charges are far rarer than small ones (Krüger et al., 2006).

If we assume, to a first order approximation, that the grain speed is nearly constant during a single stream, then the impact charge distribution derived from the stream measurements is compatible with a fairly uniform mass distribution decreasing rapidly towards heavier grains. The factor 10 variance in  $Q_1$  is consistent with the 5–10 nm-sized grains that Zook et al. (1996) argue make up jovian dust streams.

We also find differences between streams and within individual streams. The mean charge varied by up to a factor of 2 between individual streams, and scatter in the detected impact charges within a single streams was also this large or larger, making it difficult to draw any specific conclusions. Interestingly, in some streams the mean impact charge varied systematically in time, indicating an ongoing change in stream particle properties.

## 4. Analysis

### 4.1. Escape from the jovian system

The mechanism accelerating tiny particles within Jupiter’s magnetosphere to hundreds of kilometres per second has been discussed in detail in the literature (Horányi et al., 1993a, 1997; Hamilton and Burns, 1993; Horányi, 2000), and we only summarise the basic concepts here. Dust grains released from the volcanic plumes of Jupiter’s moon Io collect a net positive charge in Io’s hot plasma torus and are accelerated outward by the outward-pointing corotational electric field of the planet. Their gyroradii are sufficiently large that they are ejected from the jovian magnetosphere into interplanetary space if their sizes are in the range  $10 \text{ nm} \lesssim s \lesssim 200 \text{ nm}$  (Hamilton and Burns, 1993; Grün et al., 1998). Their escape speeds from the jovian system are up to  $300 \text{ km s}^{-1}$ , compatible with the speeds derived by Zook et al. (1996).

To a first order approximation, particles released from a source close to Jupiter’s equatorial plane are accelerated along this plane. Because Jupiter’s magnetic field is tilted by  $9.6^\circ$  w.r.t. the planet’s rotation axis, the outward acceleration also has a significant out-of-plane component.

Although the primary acceleration is radial and the particles leave the jovian system along approximately equatorial trajectories, numerical simulations show that the  $9.6^\circ$  tilt in the jovian magnetic field causes typical trajectories to bend up to  $25^\circ$  out of the plane (Horányi et al., 1997). A significant number of grains, however, can be accelerated to much higher latitudes up to  $\beta_j \simeq 90^\circ$  according to Graps (2001).

Once from Jupiter’s realm, the interplanetary electromagnetic (or Lorentz) force exceeds Solar gravity by more than a factor of 1000 for 10 nm dust grains. Accordingly, we turn now to a discussion of the Lorentz force which arises, ultimately, from plasma flowing outward in the solar wind.

### 4.2. How the interplanetary Lorentz force explains the data

The existence of the Sun’s extremely hot corona necessarily leads to the existence of a supersonic outward flow: the solar wind. The solar wind flows radially outward, in quiet times at a velocity of about  $300\text{--}500 \text{ km s}^{-1}$ , into interplanetary space carrying the solar magnetic field with it. Because the Sun is rotating, pulling the anchored footprints of the magnetic field lines with it, the magnetic field in interplanetary space forms a structure known as an Archimedian spiral (Tayler, 1997, p. 169). The spiral tightens with increasing distance and, on average, the interplanetary magnetic field vector at Jupiter lies in the ecliptic plane almost perpendicular (within  $10^\circ$ ) to the Sun–Jupiter line (Forsyth et al., 1996).

The Lorentz force is given by  $\mathbf{F} = Q\mathbf{v} \times \mathbf{B}$ , where  $Q$  is the charge on a dust grain (usually positive),  $\mathbf{B}$  is the interplanetary magnetic field, and  $\mathbf{v}$  is the speed of the dust grain relative to the magnetic field. Since the interplanetary magnetic field is being swept out of the Solar System at typical speeds of  $400 \text{ km s}^{-1}$ , somewhat faster than dust speeds,  $\mathbf{v} \approx -v\hat{\mathbf{r}}$ . Furthermore, the tangential component of the magnetic field  $B_T$  is usually observed to dominate the other components at Jupiter, in agreement with the Archimedian spiral concept discussed above. In the simplest geometries, the magnetic field switches polarity twice per solar rotation (roughly every 13 days) when the magnetic equator sweeps over Ulysses’ near-ecliptic position. Actual measurements of the magnetic field by Ulysses for this period are shown in Fig. 8 (Jones and Balogh, 2003).

Notice that  $\Phi$  in the second panel is often near  $90^\circ$  or  $-90^\circ$  in this figure, alternating every  $\sim 13$  days in reasonable agreement with the model predictions just discussed. High frequency variations are superimposed on the underlying 13-day variation, which is clearest on the left half of the panel, but still persists on the right half. Notice also the regular strengthenings of  $|\mathbf{B}|$ , the magnitude of the magnetic field vector. These are due to the so-called corotating interaction regions (CIRs) and often seem to occur near magnetic equator crossings. The fourth panel shows the normal component of the Lorentz force  $F_N$ ,



calculated using this magnetic field data and assuming a  $400 \text{ km s}^{-1}$  solar wind speed and grain charge corresponding to a potential of  $+5 \text{ V}$ . This acceleration alternates between accelerating grains primarily upward and downward with the same 13-day period.

Because the largest components of  $\mathbf{B}$  and  $\mathbf{v}$  are in the ecliptic plane, the normal component of the Lorentz force,

$F_N$ , dominates the accelerations of tiny dust grains. The simple model of Hamilton and Burns (1993) approximated the variations of  $F_N$  by a square wave with a period of half the solar rotation rate, which is a reasonable approximation to a smoothed version of the fourth panel of Fig. 8. In their analysis, a spacecraft far above or below the ecliptic plane should receive dust streams only once per solar

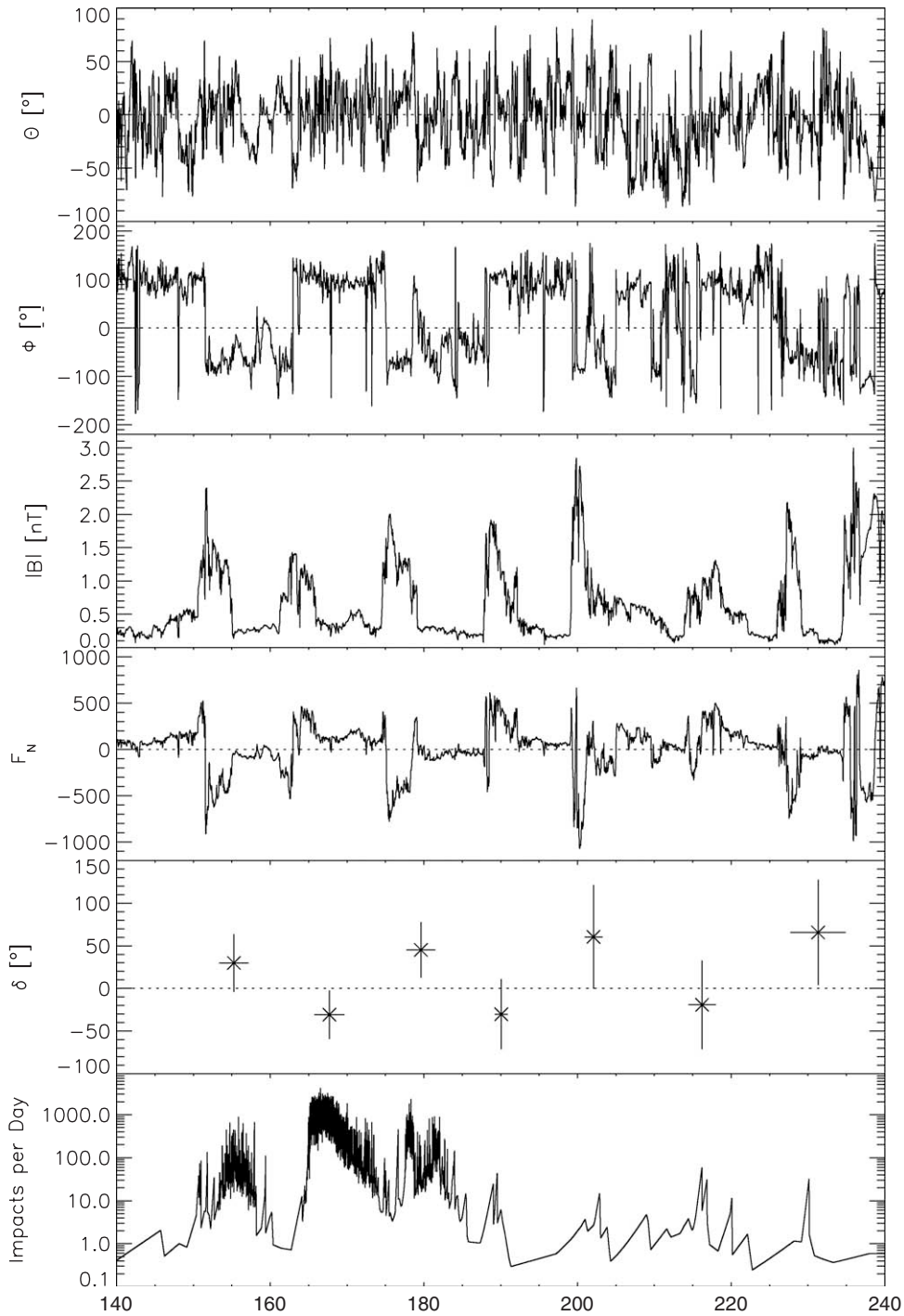


Fig. 8. Dust and magnetic field parameters for a selected period in 2004. From the top, the parameters plotted are the meridional and azimuthal angle of the magnetic field (for  $\phi \simeq 90^\circ$  the magnetic field vector is nearly parallel to Jupiter’s orbital velocity), the magnetic field strength  $|B|$ , the normal component of the Lorentz force (a constant solar wind speed has been assumed; arbitrary units), the deviation  $\delta$  of the average dust stream impact direction from the line-of-sight direction to Jupiter, and the dust impact rate.

rotation (every 26 days), while close to the plane streams should come twice as often. Hamilton and Burns (1993) suggested that these subharmonic peaks be sought and, although significantly weaker than the 26-day peaks, they were subsequently found in the 1991/92 Ulysses data (e.g. Grün et al., 2001).

We now apply this model to the current data set. When Ulysses is high above Jupiter's orbit (prior to 2004), streams need to be strongly deflected upward and this can only be accomplished during one phase of the solar rotation cycle. Thus streams are received roughly once every 26 days (see streams # 1–# 11 in Table 1). After scanning rapidly through the ecliptic, Ulysses reaches southern latitudes large enough that streams again only appear once per solar rotation; this time a large downward deflection is required to reach the spacecraft (see streams # 20–# 28 in Table 1). Between these two extremes, Ulysses is near Jupiter's orbital plane and dust initially launched with a slight upward velocity can be deflected down to Ulysses (if  $\Phi \approx 90^\circ$ ). Half a cycle later ( $\Phi \approx -90^\circ$ ), dust that happens to be launched with a slight downward velocity can be deflected back up to Ulysses. Thus there are two chances for dust to reach Ulysses per solar rotation, resulting in the more closely spaced streams # 12–# 19.

This model also predicts that the apparent direction from which dust streams appear will shift systematically depending on the phase of the solar rotation. Downward acceleration (a negative  $F_N$ ) should result in a positive  $\delta$  seen by Ulysses; exactly this correlation is visible in the fifth

panel of Fig. 8. Conversely, an upward deflection produces a negative  $\delta$ ; this provides a clear explanation for why the positive and negative deflections alternate in the fifth panel of Fig. 8.

A final feature of Figs. 5 and 6 requires explanation. Namely, why are deflection angles  $\delta$  near zero prior to 2004 when Ulysses was far above the ecliptic? Paradoxically, for dust grains to reach Ulysses at this time required a significant upward deflection. The answer comes from carefully considering the spacecraft trajectory and detector geometry. The detection geometry of the dust detector around Ulysses' aphelion passage is schematically shown in Fig. 9. Here we indicate the spacecraft trajectory projected onto a plane perpendicular to the Jupiter–Earth line in a Jupiter-centred system. The key to resolving the paradox is that only shifts in the impact direction in the  $Y'$ – $Z'$  plane are detectable by Ulysses while changes in the  $X'$ – $Z'$  plane remain undetectable. From mid 2003 through the beginning of 2004, the spacecraft was nearly in the  $X'$ – $Z'$  plane, relevant dust trajectories were roughly in this plane, and hence the shifts, also in this plane, were undetectable. The converse is true in late 2002 and in 2005 when Fig. 5 shows strong shifts and Fig. 9 predicts  $Y'$ – $Z'$  shifts that can be easily detected.

#### 4.3. Final checks of the theory

Here we critically examine some of the assertions made in the previous subsection. First, we examine the link that we have made between the measured dust stream deflection angle and the instantaneous orientation of the magnetic field at the spacecraft at the time of detection. For this to be roughly valid, dust grains must travel from Jupiter to the spacecraft rapidly compared to the solar rotation rate. Taking into account grain acceleration by the jovian magnetosphere and also in interplanetary space, 10 nm particles need about 4 days to travel 1 AU. The travel delay leads to an intrinsic shift in the magnetic field experienced by the dust grain and the spacecraft and makes comparisons of relative phases less certain for distances greater than a few AU. In addition, these time-variable forces smear out dust streams and make them more difficult to detect, especially beyond 3–4 AU from Jupiter.

Stronger magnetic fields should lead, all else being equal, to greater deflection angles  $\delta$ . In Fig. 10 we compare the deviation  $\delta$  of the dust impact direction from the line-of-sight to Jupiter with the magnetic field strength. We plot data from 2004, when Ulysses traversed a large range in jovigraphic latitude, and show the three components of the magnetic field vector in a Radial Tangential Normal (RTN) coordinate system (see also Fig. 9). We also plot the magnitude  $|B|$  of the magnetic field. There are no clear correlations with  $B_N$  and  $|B|$ , but clear—if weak—trends are seen with  $B_R$  and  $B_T$ . The component  $B_N$  is weak, and anyway, can cause no vertical accelerations; the lack of a correlation makes sense. Similarly, the absolute value  $|B|$  is not as critical as the sign of the acceleration, which is

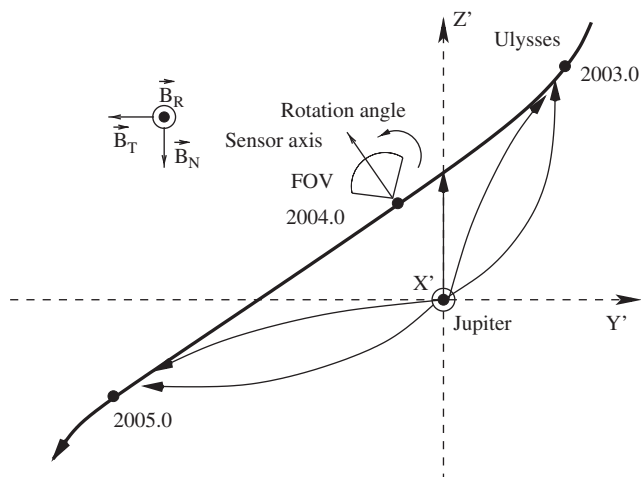


Fig. 9. Schematic sketch of the Ulysses trajectory projected onto a plane perpendicular to the Jupiter–Earth line (which coincides to within  $10^\circ$  with the Jupiter–Sun line). In the period considered in this paper, the  $Z'$  and  $Y'$  axes were roughly parallel to the  $Z$  and  $Y$  axes in Fig. 1. The negative  $X'$  axis points towards the Earth and the magnetic field vector alternates sharply between roughly the  $Y'$  and  $-Y'$  directions. Note that the dust sensor scans in the  $Y'$ – $Z'$  plane. Hence, fluctuations of the dust impact direction in the  $X'$ – $Z'$  plane remain undetectable. The field-of-view (FOV) and the scanning direction of the dust instrument are indicated. Solid lines with arrows indicate possible dust stream particle trajectories. The orientation of the magnetic field components in an RTN coordinate system are indicated (note that  $B_R$  in reality points radially outward from the Sun, not the Earth as shown here for simplicity).

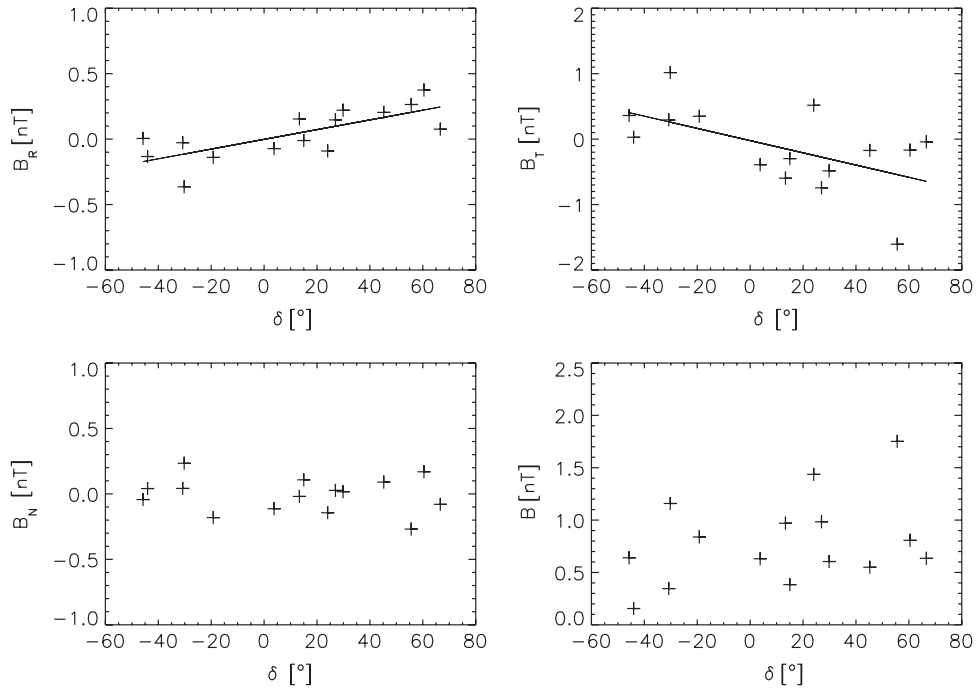


Fig. 10. Magnetic field strength ( $B_R$ ,  $B_T$ ,  $B_N$  and magnetic field magnitude  $|B|$ ) vs. deviation  $\delta$  of the average dust stream impact direction from the line-of-sight direction to Jupiter for the dust streams # 8–22 measured in 2004. In this time interval Ulysses traversed a large range in jovigraphic latitude ( $-20^\circ \leq \beta_J \leq +70^\circ$ ) with only relatively little variation in ecliptic latitude ( $-9^\circ \leq \beta_{\text{ecl}} \leq +10^\circ$ ). The solid lines are least-squares fits to the data.

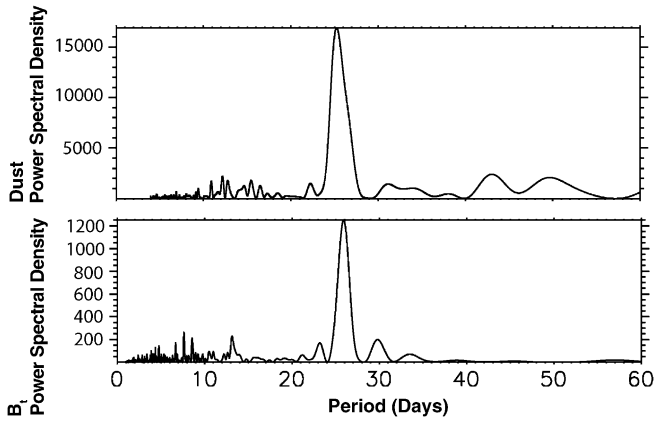


Fig. 11. Periodograms of the dust impact rate and the magnetic field data ( $B_T$  component) measured with Ulysses between day 234 in 2003 and day 328 in 2004.

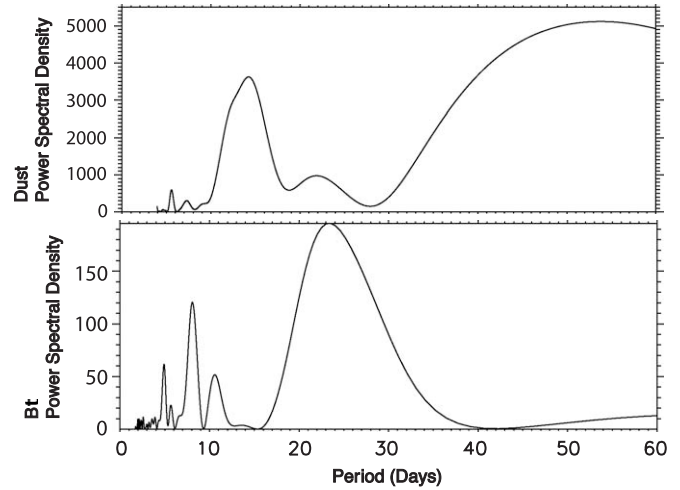


Fig. 12. Same as Fig. 11 but for the time interval day 138 to 190 in 2004.

determined by  $B_T$ . We argued above that only  $B_T$  is relevant and note that the magnetic field polarity reversals predict that  $B_R$  should correlate with  $B_T$  as observed here. No correlation is found for the 2003 data because the values for  $\delta$  cluster around  $0^\circ$  (Fig. 5) because of the spacecraft detection geometry as described above.

It should be noted that the least-squares fits to  $B_R$  vs.  $\delta$  and  $B_T$  vs.  $\delta$  pass very close to the origin of both plots. This is consistent with expectations: a very weak or absent magnetic field should not affect the particle trajectories. Although the width of the measured rotation angle distribution is relatively large due to the wide field-of-view of the dust instrument (Section 3), this result supports our

hypothesis that electromagnetic forces lead to bending of the grain trajectories.

Finally, we check the assertion that it is the long-period variation of  $B_T$  and not the high frequency noisy components that dominates the observed dynamics of dust streams (Fig. 8). In Fig. 11 we compare frequency spectra of the dust impact rate and the magnetic field measurements from Ulysses. To avoid artefacts in the spectra due to gaps in the data for the periods when the dust instrument was switched off, we only used data after summer 2003 and considered the same time interval for both data sets.

The Lomb–Scargle periodogram (Scargle, 1982) is a general linear least-squares regression of unevenly spaced data to a sine/cosine series of different frequencies. Nice features of the Lomb–Scargle periodogram are that it weighs the spectral fit appropriately by the actual data points (i.e. only at the times that the data are measured), it takes advantage that some data is clustered more tightly than the average Nyquist interval (you can pick out the higher frequencies), and it shows no aliasing.

The dust data and magnetic field data show strong peaks at  $26 \pm 2$  days and  $26 \pm 1$  days, respectively. This indicates that despite the somewhat messy appearance of the magnetic field and dust impact data in Fig. 8, it is changes at the solar rotation period that dominate, supporting the dynamical model of dust streams deflection described above. A similar analysis was used to show the importance of electromagnetic forces in the jovian system, where the relevant timescales were the jovian rotation period and half that (Grün et al., 1998; Graps et al., 2000).

In Fig. 12, we isolate a shorter period of dust data from 2004 which encompasses four dust streams occurring at roughly 13-day intervals. Because this time interval is so short, the relevant periods are not resolved very well. Nevertheless, we find that the dust data displays a strong peak at  $14 \pm 3$  days, while the magnetic field component  $B_T$  peaks at  $24 \pm 5$  days. The dust data is demonstrably different than in the previous figure, while the magnetic data is consistent with a degraded version of Fig. 11. This serves to reemphasise the fact that the difference between streams spaced by 13 and 26 days is not due to intrinsic differences in the magnetic field, but rather to Ulysses' location relative to the ecliptic plane.

## 5. Conclusions

During its distant (0.8 AU) flyby at Jupiter in 2004, the Ulysses spacecraft had its second opportunity to measure the dust streams emanating from the jovian system. Twenty-eight streams were identified in the dust data set over a 26 month period when the spacecraft was within 4 AU from Jupiter and the dust instrument was operating. During this flyby, the dust streams were measured over a large range in jovigraphic latitude  $\beta_J$  ranging from  $+75^\circ$  down to  $-25^\circ$ , more than doubling the dust stream data set. The data show clear signatures for dust particle interaction with the solar wind driven interplanetary magnetic field, confirming earlier results (Grün et al., 1993; Kempf et al., 2005).

Due to favourable detection geometry, the streams were detected about a factor of two further away from the planet. A strong dust burst lasting more than a month was measured in June/July 2004 around jovian equatorial plane crossing ( $r_J \simeq 1.3$  AU), with impact rates exceeding 2000 per day. In 1991/92 the strongest dust stream had similarly high impact rates and occurred at  $\beta_J \simeq -35^\circ$  ( $r_J = 0.26$  AU). Dust impact directions were consistent with a grain origin from the jovian system.

The dust fluxes measured above and below the jovian equatorial plane follow an inverse square drop with jovicentric distance that one expects for particle dispersion from a continuously emitting point source. This implies that systematic and stochastic variations operating within the jovian magnetosphere mostly average out in interplanetary space far away from the planet. Close to the equatorial plane, the stream fluxes were—after correction for  $r_J^{-2}$  dispersion in space—1 to 2 orders of magnitude higher than at high latitudes, for reasons that remain mysterious.

From the numerical simulations of Horányi et al. (1997) and Graps (2001) one expects particles to be transported to latitudes of  $\pm 25^\circ$  rather homogeneously while the measurements imply a much stronger concentration towards the equatorial plane. Furthermore, the analysis of Zook et al. (1996) predicts dust detections in between the dust streams which is not observed (Grün et al., 2001), although this may simply be due to the fact that Zook et al. (1996) did not constrain velocity vectors at Jupiter. Some of these velocities would, no doubt, be incompatible with a jovian origin. Additionally, forces from Jupiter's magnetic field and/or the variability of the source at Io may modulate dust streams. Enhanced volcanic activity on Io may be connected with the high dust flux measured with Ulysses in May/June 2004 (Marchis et al., 2004).

Frequency analysis revealed impact rate fluctuations with a 26-day periodicity, closely matching the solar rotation cycle. At the jovian equatorial plane the periodicity switched to about 13 days, consistent with theoretical considerations (Hamilton and Burns, 1993). The grain impact directions fluctuated with the orientation of the magnetic field vector. Close to the equatorial plane ( $-10^\circ \lesssim \beta_{\text{ecl}} \lesssim 10^\circ$ ) the impact directions of the streams are correlated with the strength of the interplanetary magnetic field vector while no such correlation is found for higher latitudes.

An additional—possibly important—phenomenon is corotating interaction regions (CIRs) which are compressed, high-speed solar wind. The magnetic field strength and, hence, the Lorentz force acting on the grains can be 5–10 times larger at these times, leading to: (i) stronger deviations from the Jupiter direction; (ii) accelerated grains and enhanced detectability and (iii) perhaps even destruction of larger grains and stream formation. The dust streams at Jupiter and Saturn are correlated with such events (Grün et al., 1993; Kempf et al., 2005). This is confirmed by the Ulysses 2002–2005 measurements: dust streams occur a few days after a CIR has been detected by Ulysses and this time delay closely matches the particle flight time from Io to the spacecraft (Flandes and Krüger, 2006). Furthermore, the duration of a stream seems to be correlated with the duration of the previously detected CIR. Perhaps CIRs compress Jupiter's magnetosphere enough to trigger a dust escape mechanism. In any case, CIRs bear further investigation as they appear to play a key role in forming or deflecting dust streams.



## Acknowledgements

We thank the Ulysses project at ESA and NASA/JPL for effective and successful mission operations. This work has been supported by the Deutsches Zentrum für Luft- und Raumfahrt e.V. (DLR) under grant 50 0N 9107. Support by the Max-Planck-Institut für Kernphysik, the Max-Planck-Institut für Sonnensystemforschung, and NASA grant NNG04GM18G is also gratefully acknowledged.

## References

- Auer, S., 2001. In: Grün, E., Gustafson, B.A.S., Dermott, S.F., Fechtig, H. (Eds.), *Interplanetary Dust*. Springer, Berlin, Heidelberg, New York, pp. 385–444.
- Baguhl, M., Grün, E., Linkert, G., Linkert, D., Siddique, N., 1993. Identification of ‘small’ dust impacts in the Ulysses dust detector data. *Planet. Space Sci.* 41, 1085–1098.
- Flandes, A., Krüger, H., 2006. CIR modulation of Jupiter dust stream detection. In: Krüger, H., Graps, A.L. (Eds.), *Proceedings of the Conference Dust in Planetary System*, held in Kauai, Hawaii, September 2005, ESA-SP, in press.
- Forsyth, R.J., Balogh, A., Smith, E.J., Erdős, G., McComas, D.J., 1996. The underlying Parker spiral structure in the Ulysses magnetic field observations, 1990–1994. *J. Geophys. Res.* 101 (10), 395–404.
- Graps, A.L., 2001. Io revealed in the Jovian dust streams. Ph.D. Thesis, Ruprecht-Karls-Universität, Heidelberg.
- Graps, A.L., Grün, E., Svedhem, H., Krüger, H., Horányi, M., Heck, A., Lammers, S., 2000. Io as a source of the Jovian dust streams. *Nature* 405, 48–50.
- Grün, E., 2001. In situ measurements of cosmic dust. In: Grün, E., Gustafson, B.A.S., Dermott, S.F., Fechtig, H. (Eds.), *Interplanetary Dust*. Springer, Berlin, Heidelberg, New York, pp. 295–346.
- Grün, E., Fechtig, H., Hanner, M.S., Kissel, J., Lindblad, B.A., Linkert, D., Maas, D., Morfill, G.E., Zook, H.A., 1992a. The Galileo dust detector. *Space Sci. Rev.* 60, 317–340.
- Grün, E., Fechtig, H., Kissel, J., Linkert, D., Maas, D., McDonnell, J.A.M., Morfill, G.E., Schwehm, G.H., Zook, H.A., Giese, R.H., 1992b. The Ulysses dust experiment. *Astron. Astrophys. (Suppl.)* 92, 411–423.
- Grün, E., Zook, H.A., Baguhl, M., Balogh, A., Bame, S.J., Fechtig, H., Forsyth, R., Hanner, M.S., Horányi, M., Kissel, J., Lindblad, B.A., Linkert, D., Linkert, G., Mann, I., McDonnell, J.A.M., Morfill, G.E., Phillips, J.L., Polansky, C., Schwehm, G.H., Siddique, N., Staubach, P., Svestka, J., Taylor, A., 1993. Discovery of Jovian dust streams and interstellar grains by the Ulysses spacecraft. *Nature* 362, 428–430.
- Grün, E., Baguhl, M., Hamilton, D.P., Kissel, J., Linkert, D., Linkert, G., Riemann, R., 1995. Reduction of Galileo and Ulysses dust data. *Planet. Space Sci.* 43, 941–951.
- Grün, E., Baguhl, M., Hamilton, D.P., Riemann, R., Zook, H.A., Dermott, S.F., Fechtig, H., Gustafson, B.A., Hanner, M.S., Horányi, M., Khurana, K.K., Kissel, J., Kivelson, M., Lindblad, B.A., Linkert, D., Linkert, G., Mann, I., McDonnell, J.A.M., Morfill, G.E., Polansky, C., Schwehm, G.H., Srama, R., 1996a. Constraints from Galileo observations on the origin of Jovian dust streams. *Nature* 381, 395–398.
- Grün, E., Hamilton, D.P., Riemann, R., Dermott, S.F., Fechtig, H., Gustafson, B.A., Hanner, M.S., Heck, A., Horányi, M., Kissel, J., Kivelson, M., Krüger, H., Lindblad, B.A., Linkert, D., Linkert, G., Mann, I., McDonnell, J.A.M., Morfill, G.E., Polansky, C., Schwehm, G.H., Srama, R., Zook, H.A., 1996b. Dust measurements during Galileo’s approach to Jupiter and Io encounter. *Science* 274, 399–401.
- Grün, E., Krüger, H., Dermott, S.F., Fechtig, H., Graps, A.L., Gustafson, B.A., Hamilton, D.P., Heck, A., Horányi, M., Kissel, J., Lindblad, B.A., Linkert, D., Linkert, G., Mann, I., McDonnell, J.A.M., Morfill, G.E., Polansky, C., Schwehm, G.H., Srama, R., Zook, H.A., 1997a. Dust measurements in the Jovian magnetosphere. *Geophys. Res. Lett.* 24, 2171–2174.
- Grün, E., Staubach, P., Baguhl, M., Hamilton, D.P., Zook, H.A., Dermott, S.F., Gustafson, B.A., Fechtig, H., Kissel, J., Linkert, D., Linkert, G., Srama, R., Hanner, M.S., Polansky, C., Horányi, M., Lindblad, B.A., Mann, I., McDonnell, J.A.M., Morfill, G.E., Schwehm, G.H., 1997b. South–North and radial traverses through the interplanetary dust cloud. *Icarus* 129, 270–288.
- Grün, E., Krüger, H., Graps, A., Hamilton, D.P., Heck, A., Linkert, G., Zook, H., Dermott, S.F., Fechtig, H., Gustafson, B., Hanner, M., Horányi, M., Kissel, J., Lindblad, B., Linkert, G., Mann, I., McDonnell, J.A.M., Morfill, G.E., Polansky, C., Schwehm, G.H., Srama, R., 1998. Galileo observes electromagnetically coupled dust in the Jovian magnetosphere. *J. Geophys. Res.* 103, 20011–20022.
- Grün, E., Krüger, H., Landgraf, M., 2001. Cosmic dust. In: Balogh, A., Marsden, R., Smith, E. (Eds.), *The Heliosphere at Solar Minimum: The Ulysses Perspective*. Springer, Praxis, Berlin, pp. 373–404.
- Hamilton, D.P., Burns, J.A., 1993. Ejection of dust from Jupiter’s gossamer ring. *Nature* 364, 695–699.
- Horányi, M., 2000. Dust streams from Jupiter and Saturn. *Phys. Plasmas* 7 (10), 3847–3850.
- Horányi, M., Morfill, G.E., Grün, E., 1993a. Mechanism for the acceleration and ejection of dust grains from Jupiter’s magnetosphere. *Nature* 363, 144–146.
- Horányi, M., Morfill, G.E., Grün, E., 1993b. The dusty ballerina skirt of Jupiter. *J. Geophys. Res.* 98, 21245–21251.
- Horányi, M., Grün, E., Heck, A., 1997. Modeling the Galileo dust measurements at Jupiter. *Geophys. Res. Lett.* 24, 2175–2178.
- Jones, G.H., Balogh, A., 2003. The global heliospheric magnetic field polarity distribution as seen at Ulysses. *Ann. Geophys.* 21, 1377–1382.
- Kempf, S., Srama, R., Horányi, M., Burton, M.E., Helfert, S., Moragas-Klostermeyer, G., Roy, M., Grün, E., 2005. High-velocity streams of dust originating from Saturn. *Nature* 433, 289–291.
- Krüger, H., Grün, E., Heck, A., Lammers, S., 1999. Analysis of the sensor characteristics of the Galileo dust detector with collimated Jovian dust stream particles. *Planet. Space Sci.* 47, 1015–1028.
- Krüger, H., Geissler, P., Horányi, M., Graps, A.L., Kempf, S., Srama, R., Moragas-Klostermeyer, G., Moissl, R., Johnson, T.V., Grün, E., 2003. Jovian dust streams: a monitor of Io’s volcanic plume activity. *Geophys. Res. Lett.* 30, 2101–2105.
- Krüger, H., Grün, E., Linkert, D., Linkert, G., Moissl, R., 2005. Galileo long-term dust monitoring in the jovian magnetosphere. *Planet. Space Sci.* 53, 1109–1120.
- Krüger, H., Altobelli, N., Anweiler, B., Dermott, S.F., Dikarev, V., Fechtig, H., Graps, A.L., Grün, E., Gustafson, B.A., Hamilton, D.P., Hanner, M.S., Horányi, M., Kissel, J., Landgraf, M., Lindblad, B., Linkert, D., Linkert, G., Mann, I., McDonnell, J.A.M., Morfill, G.E., Polansky, C., Schwehm, G.H., Srama, R., Zook, H.A., 2006. Five years of Ulysses dust data: 2000 to 2004. *Planet. Space Sci.*, in press.
- Marchis, F., Davies, A.G., Gibbard, S.G., Le Mignant, D., Lopes, R.M., Macintosh, B., de Pater, I., *Volcanic Activity of Io Monitored with Keck-10m AO in 2003–2004*, AGU Fall Meeting Abstracts, 2004, C1483+
- Oberst, J., Nakamura, Y., 1991. A search for clustering among the meteoroid impacts detected by the Apollo Lunar Seismic Network. *Icarus* 91, 315–325.
- Postberg, F., Kempf, S., Green, S.F., Hillier, J.K., McBride, N., Grün, E., 2006. Composition of jovian dust stream particles. *Icarus*, in press.
- Scargle, J.D., 1982. Studies in astronomical time series II: statistical aspects of spectral analysis of unevenly spaced data. *Astrophys. J.* 263, 835–853.
- Taylor, R.J., 1997. *The Sun as a Star*. Cambridge University Press, Cambridge.
- Wenzel, K., Marsden, R., Page, D., Smith, E., 1992. The Ulysses mission. *Astron. Astrophys. (Suppl.)* 92, 207–219.
- Willis, M.J., Burchell, M., Ahrens, T.J., Krüger, H., Grün, E., 2005. Decreased values of cosmic dust number density estimates in the solar system. *Icarus* 176, 440–452.
- Zook, H.A., Grün, E., Baguhl, M., Hamilton, D.P., Linkert, G., Linkert, D., Liou, J.-C., Forsyth, R., Phillips, J.L., 1996. Solar wind magnetic field bending of Jovian dust trajectories. *Science* 274, 1501–1503.